JOURNAL OF PHYSIOLOGY AND PHARMACOLOGY 2005, 56, Supp 3, 159–179
www.jpp.krakow.pl

M. LAMPARSKA-PRZYBYSZ [1], B. GAJKOWSKA [2], T. MOTYL [1]

CATHEPSINS AND BID ARE INVOLVED IN THE MOLECULAR SWITCH BETWEEN APOPTOSIS AND AUTOPHAGY IN BREAST CANCER MCF-7 CELLS EXPOSED TO CAMPTOTHECIN

[1]Department of Physiological Sciences, Faculty of Veterinary Medicine, Warsaw Agricultural University, Warsaw, Poland
[2]Department of The Cell Ultrastructure, Medical Research Center, Polish Academy of Sciences, Warsaw, Poland

The details of molecular switching points between apoptosis and autophagy in tumor cells have still not been fully elucidated. This study focused on the role of cathepsin B and its substrate, BID as molecular links between apoptosis and autophagy in human breast cancer MCF-7 cells exposed to camptothecin. Apoptosis occurred rapidly with a peak in 60 min after drug administration, whereas autophagy developed at a much slower rate with continuous progression during 24 h of cell exposure to the drug. CPT induced very rapid activation of cathepsin B. Inhibition of cathepsins by E64d prevented CPT-induced BAX and BID aggregation on mitochondria and reduced significantly reduced apoptotic cell number. The above effects were accompanied by an increase in autophagosome formation, measured by expression of MAP I LC3. BID knock down resulted in strong suppression of CPT-induced apoptosis and a shift of cell death towards autophagy, manifesting with an increase of Beclin 1 and MAP I LC3 cellular content.

Key words: *apoptosis, autophagy, Beclin 1, BID, cathepsin B, MAP I LC3, breast cancer, camptothecin*

INTRODUCTION

Cells use different pathways to activate self-destruction processes. There are five types of Programmed Cell Death (PCD): type I or apoptosis, which is

dependent on the activity of caspases, type II - autophagy, type III - anoikis, type IV - amorphosis and type V - mitotic catastrophe (1).

Apoptosis is a rapid and precisely controlled type of PCD involving a complex of signaling molecules, regulatory proteins (e.g. BCL-2 death promoters and inhibitors), mitochondrial mediators (cytochrome c, Smac/DIABLO, Omi/HtrA2, AIF) and death executors (caspases, calpains, DNases). It is commonly accepted that the most characteristic biochemical feature of apoptosis is the activation of caspases and oligonucleosomal fragmentation of DNA resulting in a lowered nuclear DNA content (Sub - G1-region on DNA histogram) (2).

Phylogenetically, autophagy is a very old process, usually considered to be a route for cellular protein degradation and organelle turnover, comprising macroautophagy, microautophagy, and chaperone-mediated autophagy (3, 4). For these reasons, autophagy is beneficial in maintaining homeostasis and cell survival. On the other hand, autophagy is also involved in eliminating cancer cells by triggering a non-apoptotic cell death program (PCD II), indicating a role in counteracting tumor development (1, 5-7). Yeast genetics revealed two *ubiquitin-like* conjugation systems in autophagosome formation: 1) a system mediating the conjugation of Atg12 - Atg5 proteins and 2) a system producing covalent linkage between Atg8 and phosphatidylethanolamine (5, 8). The autophagic process in mammalian cells is regulated by homologs of the ATG and AUT family of yeast genes. Beclin 1, a homolog of the yeast autophagy protein Atg6, is required for vacuolar transport and can induce autophagy in human cells (3). The mammalian homolog of the yeast *Atg8* gene codes microtubule-associated protein I (MAP I) light chain 3 (LC3), which is bound with autophagic membranes and is currently the only reliable marker of autophagosomes (8-11).

Increasing evidence suggests that lysosomes are important mediators of PCD. In autophagic cell death lysosomes fuse with autophagosomes to form autophagolysosomes in which the cell contents are degraded (12). In apoptosis cathepsins are released from lysosomes into the cytoplasm and trigger a cascade of intracellular degradation (13-16). The key to understanding these events seems to be the mechanism controlling the release of cathepsins from lysosomes. During salt-induced hepatic apoptosis selective translocation of cathepsin B to the cytosol and nucleus is observed (17). On the other hand, this mechanism depends on a quantitative relationship between the amount of lysosomal rupture and the modulation of cell death. Low stress triggers limited release of lysosomal enzymes into the cytoplasm followed by apoptotic death, but extensive damage may induce massive lysosomal rupture and rapid cellular necrosis (18).

Cathepsins trigger apoptosis via a number of pathways. These enzymes may directly attack mitochondria and induce membrane permeabilization and cytochrome c release (15). Cathepsins can also, directly or indirectly, induce formation of mitochondrial ROS, which may cause oxidant-induced lysosomal destabilization (13). Cathepsins can activate promoters of apoptosis from the Bcl-2 family, e.g. BAX is activated by cathepsin D through proteolytic cleavage (15,

19-20). Cathepsins (particularly cathepsin B) can also activate BID by its cleavage at Arg65 or Arg71, which was shown in tumor cells (14) and cell-free extracts from NT2 cells (19). Cathepsins (e.g. cathepsin B) can directly cleave caspase zymogenes and caspases, e.g. caspase-3 (21). There is also evidence of the involvement of cathepsin B in the caspase-8-dependent apoptotic signaling cascade triggered by TNFα (22). Release of proteolytic enzymes from lysosomes may activate lytic pro-enzymes, such as PLA2, which can attack both mitochondria and lysosomes (23). Induction of the tumor suppressor protein p53 can also participate in early lysosomal membrane permeabilization and release of apoptosis-inducing enzymes (24).

Despite intensive study, the relationship between molecular mechanisms of apoptosis and autophagy in tumor cells has not been well described. This study focused on the role of cathepsin B and its substrate BID as molecular links between apoptosis and autophagy, as well as on the complementarity of both cell death types in breast cancer MCF-7 cells exposed to the cytostatic drug, camptothecin (inhibitor of DNA topoisomerase I). Laser scanning cytometry, homeostatic confocal microscopy, MicroImage System, and transmission electron microscopy were used to examine apoptosis, autophagy, cathepsin B activation, and BAX and BID aggregation within tumor cells. The RNAi technique was used for silencing BID expression and to investigate its role as a molecular switch between the apoptotic and autophagic pathways.

MATERIALS AND METHODS

Media and reagents

DMEM medium with L-glutamine and sodium pyruvate, phosphate buffered saline, pH = 7.4 (PBS), FCS, fungizone, and gentamycin sulphate were obtained from Gibco BRL (Paisley, Scotland). Bid siRNA (10 mM) and polyclonal goat anti-Bid, goat anti-MAPI LC3, goat anti-Beclin 1, rabbit anti-PARP and donkey anti-goat HRP were supplied by Santa Cruz Biotechnology Inc. (Santa Cruz, CA, USA). Monoclonal mouse anti-Bax was purchased from Oncogene Research Products (San Diego, CA, USA). Alexa Fluor 488 chicken anti-goat secondary antibody, Alexa Fluor 488 chicken anti-mouse secondary antibody, and Alexa Fluor 488 chicken anti-rabbit secondary antibody were from Molecular Probes (Eugene, OR, USA). Donkey anti-goat H+L gold conjugated 18 nm was obtained from Jackson ImmunoResearch Laboratories Inc. (West Grove, PA, USA). Camptothecin and other chemicals were from Sigma Chemical Corp. (St. Louis, MO, USA). Sterile conical flasks, 8-chamber culture slides and sterile disposable pipettes were purchased from Nunc Inc. (Naperville, IL, USA). Caspase 8 inhibitor Z-Ile-Glu(O-Me)-Thr-Asp(O-Me) fluoromethyl ketone (z-IETD-FMK), calpain inhibitor I (ALLN), cathepsins inhibitor (E64d) and TNF-α were from Sigma Chemical Corp. (St. Louis, MO, USA). LipofectAMINE Reagent and PLUS Reagent, and geneticin (G418) were from Gibco BRL (Paisley, Scotland). pDsRed2 - Mito Vector was from Clontech (Paolo Alto, CA, USA) and pEGFP-Bax Vector was kindly provided by Professor Bozena Kaminska-Kaczmarek (Nencki Institute of Experimental Biology, Warsaw, Poland). Cathepsin B substrate Magic Red® was purchased from ICN Biomedicals, Inc. (Irvine, CA, USA). Reagents for Western blotting were purchased from BioRad (Hercules, CA USA) and

Western blotting detection reagents and Hyperfilm ECL were from Amersham Pharmacia Biotech (Little Chalfont, UK).

Cell culture

Human breast cancer cell line MCF-7 was obtained from the American Type Culture Collection (Rockville, MD, USA). Cell cultures were maintained in DMEM supplemented with 10% (v/v) FCS, 50 μg/ml gentamycin, 2.5 μg/ml fungizone, 50 UI/ml penicillin and 50 μg/ml streptomycin in an atmosphere of 5% CO_2 / 95% humidified air at 37°C, and routinely subcultured every 2 or 3 days.

Drugs

Camptothecin (CPT) was diluted in DMSO to create a stock solution that was stored according to the manufacturers' suggestions. The final solution used in the experiments was 0.15 μM. This concentration of CPT was selected on the basis of our previous experiments on MCF-7 cells (25) and other tumor cells (26-27).

Inhibitors, substrates and apoptotic factors

Z-Ile-Glu(O-Me)-Thr-Asp(O-Me) fluoromethyl ketone (z-IETD-FMK), and calpain Inhibitor I (ALLN) were used at concentrations of 25 μM, papain-like cystein protease inhibitor (E64d), at 15 μM. MCF-7 cells were incubated with z-IETD-FMK for 30 min or with ALLN and E64d for 3 h prior to CPT treatment. In experiments with CPT-induced cathepsin B activation, the Magic Red® substrate was used for 15 min after preincubation with inhibitors and CPT exposition for 1, 3, 6, 12 or 24 h, respectively. Homeostatic confocal microscopy was used to analyze the kinetics of cathepsin B activation and release to the cytoplasm. The Magic Red® substrate was used in these experiments at a concentration according to the producer's protocol. MCF-7 cells were preincubated for 30 min with Magic Red® substrate before administration of CPT to the growth medium. To compare cathepsin B activation in extrinsic and intrinsic apoptosis pathways, MCF-7 cells were incubated for 1h with CPT (0.15 μM) or TNF-α at a concentration of 10 ng/ml, respectively, before administration of cathepsin B substrate.

Transfection

MCF-7 cells were transfected using lipofectAMINE Reagent and Reagent PLUS and pEGFP-BAX. The cells were incubated under optimal conditions until 70% confluency. Then the transfection solution was prepared as follows: in one tube 2 μg of DNA and 4 μl of Regent PLUS were diluted into 0.1 ml serum-free medium, in the second tube, 15 μl of lipofectAMINE Reagent were diluted into 0.1 ml serum-free medium. Both solutions were carefully combined and the obtained mixture was incubated at room temperature for 30 min. The cells were then washed and overlaid with 0.8 ml of serum-free medium and the transfection mixture was added dropwise and incubated at 37°C, under a 5% CO_2 atmosphere over the next 3 h. Afterwards, the transfection medium was supplemented with FCS to a final concentration of 10%. After 48 h transfected cells were selected using geneticin (400 μg/ml). After 2 weeks the obtained culture was transfected with pDsRed2 - Mito Vector following the same procedure. For Bid knock-down, MCF-7 cells were transfected using lipofectAMINE 2000 Reagent Bid siRNA. The cells were incubated on 8-chamber culture slides under optimal conditions until 70% confluency. Then the transfection solution was prepared: in one tube 2.5 μl of siRNA were diluted into 0.05 ml serum free medium, in the second tube, 2.5 μl of lipofectAMINE Reagent were diluted into 0.05 ml serum-free medium. Both solutions were carefully combined and the obtained mixture was incubated at room temperature for

30 min. The cells were then washed and overlaid with 0.25 ml of serum free medium and the transfection mixture was added dropwise and incubated at 37°C under a 5% CO_2 atmosphere over the next 5 h. Afterwards the transfection medium was changed to growth medium (10% FCS/DMEM). After 24 h the experimental medium with CPT (0.15 μM) was added to the cultures and the cells were incubated for 1, 3, 6, 12 or 24 hours.

Experimental procedure and immunofluorescence staining

Exponentially growing cells were plated on 8-chamber culture slides, cultured for 24 h and then incubated with the drug in 10% FCS/DMEM for up to 6 h. The control cultures were treated with equivalent concentrations of DMSO suspended in 10% FCS/DMEM. Then cells were fixed in 0.25% formaldehyde for 15 min, washed twice with PBS, suspended in ice-cold 70% methanol and stored at 2°C for 30 min. Afterwards methanol was aspirated, and samples were stored at -80°C until staining. The cells were washed twice with PBS-1% BSA and incubated for 1 h with either primary antibody diluted 1:250 with PBS-1% BSA. After primary incubation the cells were washed twice with PBS-1% BSA, and incubated for 1 h with 1:500 secondary antibodies. The cells were then washed twice in PBS-1% BSA and finally incubated with a 5 μg/ml solution of 7-aminoactinomycin D (7-AAD) for 30 min to counterstain the DNA. Then the chamber walls were removed and coverslips were mounted on microscope slides using an anti-fade mounting medium (ICN Biomedicals inc., Aurora, OH, USA).

Laser scanning cytometry

Probes were analyzed by laser scanning cytometer (LSC) (CompuCyte Corp., Boston, MA, USA). At least $5x10^3$ cells per chamber area were analyzed. The fluorescence excitation was provided by a 488 nm, 10 mW Argon laser beam. The green fluorescence of Alexa Fluor 488-labeled antibody was measured using a combination of dichroic mirrors and filters transmitting at 520 ± 20 nm (detector offset and gain set to 2000 and 32, respectively), and far red fluorescence of 7-AAD transmitting at >650 nm (offset 2000 and gain 30). The percentage of apoptotic cells was measured as the percentage of cells with a lower concentration of DNA (Sub - G1 region). Another measured parameter was the maximal pixel of BAX and BID fluorescence (MP) corresponding to the highest value of fluorescence in the cell, regardless of the cellular compartment. The obtained results were analyzed by Prism version 2.0 software (GraphPad Software, San Diego, CA).

Confocal microscopy and homeostatic confocal microscopy

For the immunostaining experiments cells were cultured on 8-chamber culture slides and measured with the combinations of excitation/emission: Argon 488 nm laser vs. 505-525 nm filter for Alexa 488, and HeNe 543 nm laser vs. 610 nm filter for 7-AAD and cathepsin B substate.

For the experiments conducted with the use of living cells the confocal microscope was equipped with a special homeostatic chamber (Solent Scientific Ltd, Portsmouth, UK) allowing standard growing conditions for the cells over the experimental period (37°C, 5% CO_2, 95% humidified air). Transfected cells were cultured on coverglass-mounted-4-chamber culture dishes. Cells were measured with the combinations of excitation/emission: Argon 488 nm laser vs. 505-525 nm filter for GFP, and HeNe 543 nm laser vs. 610 nm filter for RFP and cathepsin B substate. The experimental data was gathered from one-cell 3D reconstructions at 30 s intervals for 20 min. Then CPT (final concentration of 0.15 μM) was added to the medium and the cells were observed over the next 60 - 120 min.

Postembedding Immunogold Labeling

The cells were fixed in 4% paraformaldehyde and 0.1% glutaraldehyde in 0.1 M PBS for 2 h at 4°C. The cells were washed in PBS overnight, treated with 1% OsO_4 for 30 min, dehydrated in an ethanol gradient, and then embedded in Epon 812. Ultrathin sections were processed according to the postembedding immunogold procedure: mounted on formvar-coated nickel grids, incubated in 10% hydrogen peroxide for 10 min, rinsed in distilled water and PBS for 15 min, and blocked for 15 min in 1% bovine serum albumin (BSA) in PBS.

The labeling was performed with the use of goat anti-cathepsin B antibody (1:200). The sections were incubated for 2 h at 37°C. Secondary antibodies used in the experiment were colloidal gold-conjugated donkey anti-goat 18 nm. They were applied for 1 hour at 37°C at a dilution of 1:50.

The sections were rinsed in PBS and distilled water prior to the counterstaining with uranyl acetate and lead citrate and examined in a JEOL 1200 EX electron microscope.

The negative control immunoelectron microscopy was performed with irrelevant primary antibodies followed by the corresponding secondary anti-goat labeled antibodies as specified above. These controls demonstrated no labeling.

Transmission electron microscopy of Epon-embedded cells

Cells were fixed in mixture 2.5% glutaraldehyde in 0.1 M cacodylic buffer, pH 7.4 for 2 hours at 4°C, washed in 0.1 M cacodylic buffer, pH 7.4, overnight, and postfixed with 1% osmium tetroxide with 0.8% K_4FeCN_6 in cacodylic buffer for 1 hour at room temperature. The material was dehydrated in an ethanol gradient (30, 50, 70, 80, 90, 96, and 100 %) and propylene oxide and embedded in Epon 812. The blocks were cut with an LKB - Nova microtome and stained with 9% uranyl acetate and Reynolds solution. Samples were photographed in a JEOL 1200 EX electron microscope at 80 kV.

Western blot analysis

Cells were cultured in sterile conical flasks, or in Petri dishes in a 10% FCS/DMEM culture medium until they reached 90% confluence. To knock-down the *bid* gene, medium was removed and replaced with the transfection medium with BID siRNA, as described earlier. On the next day the control (BID (+)) and *bid*-silenced (BID (-)) cells were exposed to experimental medium with CPT (0.15 μM) for 6, 12 or 24 h. The cultured cells were centrifuged at 2000 g, for 5 min, at 4°C and the remaining pellet was used for subsequent analyses. Samples were kept frozen at -80°C until the isolation of proteins. At the time of analysis the cells were suspended in ice-cold PBS. After centrifugation the supernatant was removed and the cell pellet was resuspended in 0.5 ml Lysis Buffer RIPA prepared according to the research application from Santa Cruz Biotechnology, and incubated at 4°C for 30 min. The cells suspended in the buffer were centrifuged at 9000 g, 10 min, at 4°C, then the supernatant (containing the total protein fraction) was carefully removed and passed six times through a 20-gauge syringe needle. The lysates were mixed 1:2 (v/v) with Laemmli sample buffer (BioRad) containing 2.5% 2-mercaptoethanol and boiled for 3 min.

Samples containing identical quantities of proteins were subjected to SDS-PAGE (12% gel) together with a Kaleidoscope Marker (BioRad). The electrophoresis was run for 1 hour at 100 V using a Mini Protean II ™ cell (BioRad). After electrophoresis the separated proteins were electroblotted on a PVDF membrane (Amersham Pharmacia Biotech) for 70 min at 110 V using the Mini Protean II ™ cell. The membranes were blocked overnight with 5% w/v solution of non-fat powdered milk in TBST (pH 7.5). The following day the membranes were rinsed three times for 10 min in TBST, at room temperature, and then incubated for 1 hour at room temperature with the primary antibodies diluted 1:400. The membranes were then rinsed four times for 10 min in TBST and incubated with diluted

1:2500 secondary antibodies conjugated with horseradish peroxidase for another 1 h at room temperature. Finally, the membranes were rinsed three times for 10 min in TBST, and labeled proteins were visualized using the ECL Western blotting detection reagent on a high performance chemiluminescence Hyperfilm ECL (Amersham Pharmacia Biotech). The image on hyperfilm was then analyzed with a Kodak Edas System and the integrated optical density (IOD) was measured.

Statistical evaluation

The results were statistically evaluated by ANOVA and Tukey's multiple range tests using Prism version 2.0 software (GraphPad Software, San Diego, CA); $p \leq 0.05$ was regarded as significant and $p \leq 0.01$, as highly significant.

RESULTS

Apoptosis and autophagy are complementary forms of PCD in MCF-7 breast cancer cells exposed to CPT

MCF-7 breast cancer cells exposed to an inhibitor of DNA topoisomerase I, camptothecin (CPT), were used as an experimental model. MCF-7 cells are very useful in the study of apoptosis-autophagy relationships because they may enter both the apoptotic and the autophagic pathway of cell death, as has been shown in several experiments (2, 16). The concentration of CPT used in the study (0.15 μM) was selected on the basis of our previous experiments (25-27).

Quantitative evaluation of apoptosis was performed with LSC by analysis of DNA frequency distribution histograms, where the Sub-G1 region corresponded to apoptotic cells. It has been shown that breast cancer MCF-7 cells grown even under optimal conditions (10 % FCS/DMEM) undergo spontaneous apoptosis at the level of 4.23 ± 0.5%. Administration of CPT (0.15 μM) had a highly significant effect and increased the number of apoptotic cells to 18.7 ± 1.25%; 28.7 ± 4% and 20.4 ± 2.24% after 30, 60 and 180 min, respectively (*Fig. 1*). Evaluation of autophagy was performed through analysis of microtubule-associated protein I (MAP I) light chain 3 (LC3) expression, which is currently the only reliable marker of autophagosomes (3, 28). The expression of MAP I LC3 in breast cancer MCF-7 cells increased by 64 ± 9.5%; 99 ± 12.5% and 224 ± 25% (percentage of control cells) after 3, 6 and 24 h of CPT treatment, respectively. This indicates that CPT-induced autophagy occurs in parallel with apoptosis, however, at a considerably slower rate (*Fig. 1*). The peak of apoptosis appeared after 60 min of cell exposure to CPT, whereas the expression of the autophagy marker, MAPI LC3, increased progressively throughout the 24 h-observation period in the surviving cells. Since the number of cells decreased in the course of CPT treatment due to detachment, the increased expression of MAPI LC3 probably concerned the apoptosis-resistant cell subpopulation.

Ultrastructural analysis of the CPT-treated MCF-7 cells revealed typical morphological features of apoptosis like: cell shrinkage, plasma membrane

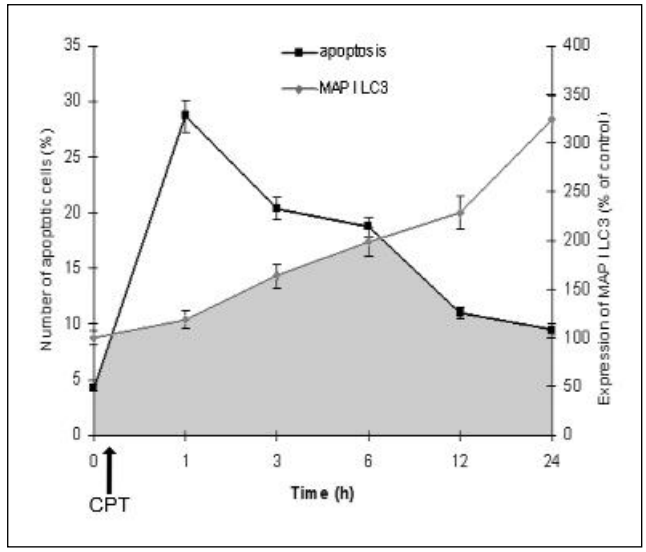

Fig. 1. Effect of CPT (0.15 μM) on apoptosis and autophagy in human breast cancer MCF-7 cells. Apoptosis was evaluated by measurement of cell number in the sub - G1 region on DNA histograms, whereas autophagy by analysis of MAP I LC3 expression and presented as a percentage of control (untreated cells). Grey area under the curves indicates the coexistence of both PCD types. Each point represents the mean (± SE) from 6 replications of 3 different experiments.

blebbing, condensation of cytoplasm and chromatin, fragmentation of the rough endoplasmic reticulum (RER), loss of ribosomes, and changes in mitochondrial ultrastructure. We also found cells sharing morphological features of apoptosis and autophagy (*Fig. 2 b, c, d*), indicating the possibility of coexistence of both PCD types. These cells exhibited the condensation and margination of chromatin that is characteristic of apoptosis, but also typical characteristics of autophagy-autophagic double-membraned giant autophagolysosomes containing cytoplasmic fragments and preserved organelles like: RER, mitochondria, dense bodies, lysosomes and ribosomes (*Fig. 2b, c*). At more advanced stages the autophagic vacuoles contained disintegrated cellular structures. Among such cells, cells with typical features of autophagy like: nuclei with centrally condensed chromatin, very well-developed Golgi complex, heavily vacuolized cytoplasm, with a few short channels of RER, and abundant free ribosomes were present (*Fig. 2d*).

Kinetics of cathepsin B activation in CPT-induced apoptosis

Since the lysosomal proteases are involved both in apoptosis and autophagy, they (or their targets) may serve as molecular links between both PCD types in tumor cells. In the first step, the kinetics of cathepsin B activation by CPT was investigated in living cells by homeostatic confocal microscopy 3D reconstruction (see Materials and Methods). A progressive increase of cathepsin B activity and release to the cytoplasm was observed within 24 min after administration of CPT to the incubation medium (with Magic Red® substrate), which was manifested with a higher intensity and dissemination of cathepsin B product-related red fluorescence (*Fig. 3*).

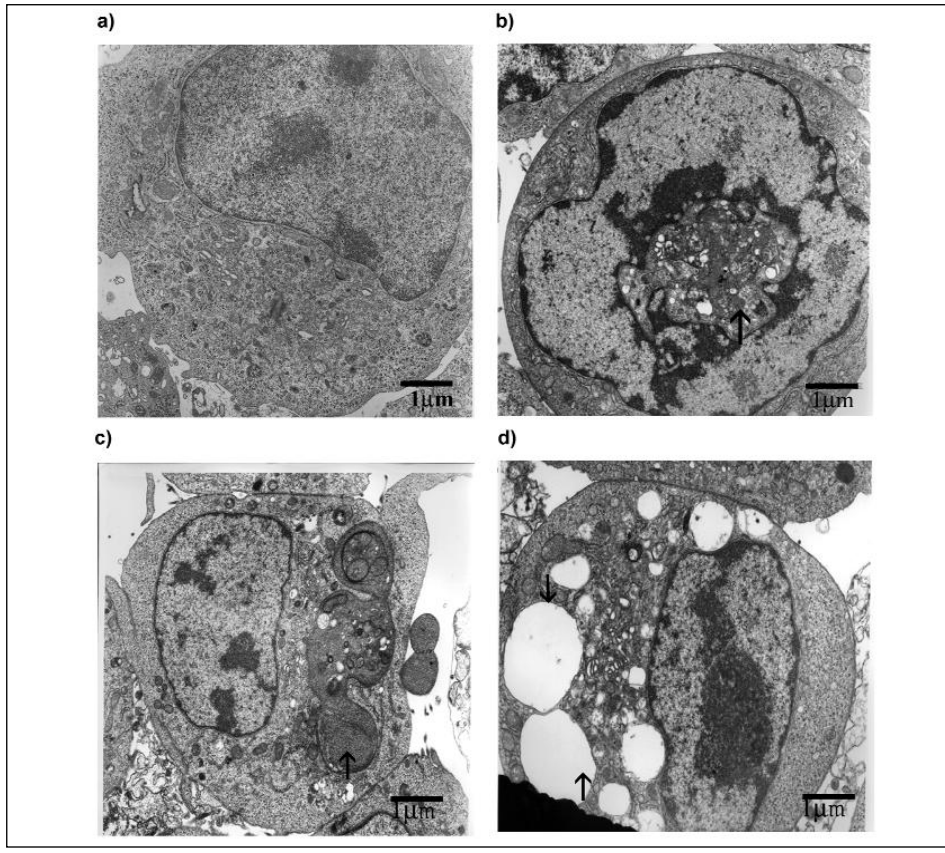

Fig. 2 Electron microscopy images showing ultrastructural features of a control cell (a) and coexistence of morphological features of apoptosis and autophagy in MCF-7 cells exposed to CPT (0.15 µM) for 6h: (b, c, d).
a) The cell exhibits the characteristic ultrastructural morphology of a control cell. The uniform nucleus is composed of regular dispersed chromatin and two nucleoli. Cytoplasm rich in RER is filled with ribosomes, polyribosomes and mitochondria. The well-developed Golgi complex is located in the cytoplasm in perinuclear areas. Scarce, dense bodies and occasional autolysosomes are present in the cytoplasm. Bar = 1 µm. *b)* The cells contain giant autophagosomes (feature of autophagy) distributed throughout the cytoplasm (arrow). Engulfed organelles in the autophagosome display degenerative alterations. Note deeply invaginated, irregular nucleus with condensed chromatin along the nuclear envelope and condensed cytoplasm (feature of apoptosis). Bar = 1 µm. *c)* The cell displays plasma membrane blebbing, (asterix) and partially condensed chromatin in an oval, pyknotic nucleus as morphological features of apoptosis. In the cytoplasm, double-membraned giant autophagic vacuoles (ultrastructural feature of autophagy) contain a large part of the cytoplasm with some preserved organelles like RER, mitochondria, dense bodies, ribosomes (arrow). Bar = 1 µm. *d)* The cell contains an oval, pyknotic nucleus with central condensed chromatin (characteristic ultrastructural feature of autophagy). In heavily vacuolized cytoplasm (arrows), prominent Golgi complex with numerous coated, smooth, and small electron dense vesicles are seen. Note scarce short channels of RER and areas of cytoplasm filled with free ribosomes and completely absent polyribosomes and ultrastructurally unchanged mitochondria. Bar = 1 µm.

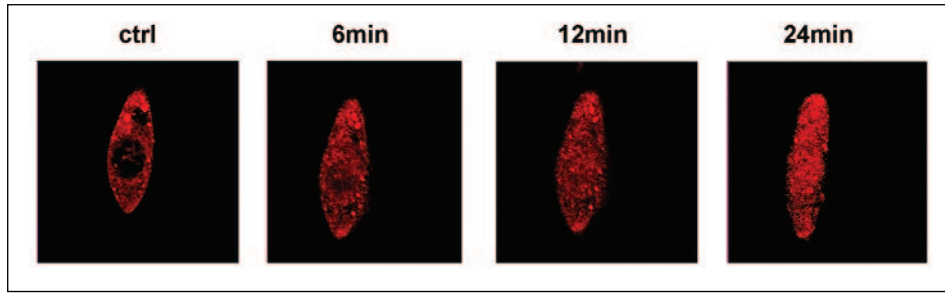

Fig. 3. Effect of CPT (0.15 μM) on activation and subcellular redistribution of cathepsin B in human breast cancer MCF-7 cells. The kinetics of cathepsin B activation shown by Magic Red® substrate - related red fluorescence.

The release of cathepsin B to the cytosol under the influence of CPT was confirmed by immunoelectron microscopy showing cathepsin B-related gold particles localized in the cytosol and nucleus within 30 min after drug administration (*Fig. 4*). In the cytoplasm, gold particles representing cathepsin B (18 nm diameter) were found as clusters or alone in close association with membranes of the RER, plasma membrane and nuclear envelope. Some lysosomes and autophagic vacuoles of damaged mitochondria were also decorated by gold particles (*Fig.4a*). The gold particles representing cathepsin B were present in the nucleoplasm within the nucleus and very often near the nuclear pore (*Fig. 4b*).

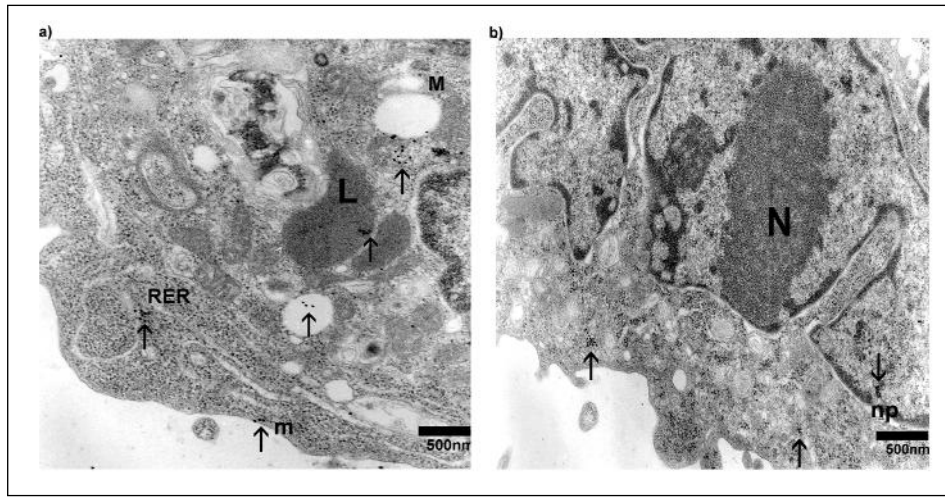

Fig. 4. Immunoelectron microscopical localization of cathepsin B; The aggregation of gold particles (18 nm) representing cathepsin B (arrows) on RER, plasma membrane (m), lysosomes (L) and damaged mitochondrium (M) are present. Bar = 500 nm.
a) immunoelectron microscopical localization of cathepsin B; Aggregates or simple gold particles representing cathepsin B in nucleus and cytoplasm are seen (arrows). Note aggregates of gold particles in the area of nucleoplasm near nuclear pore (np). Bar = 500 nm.

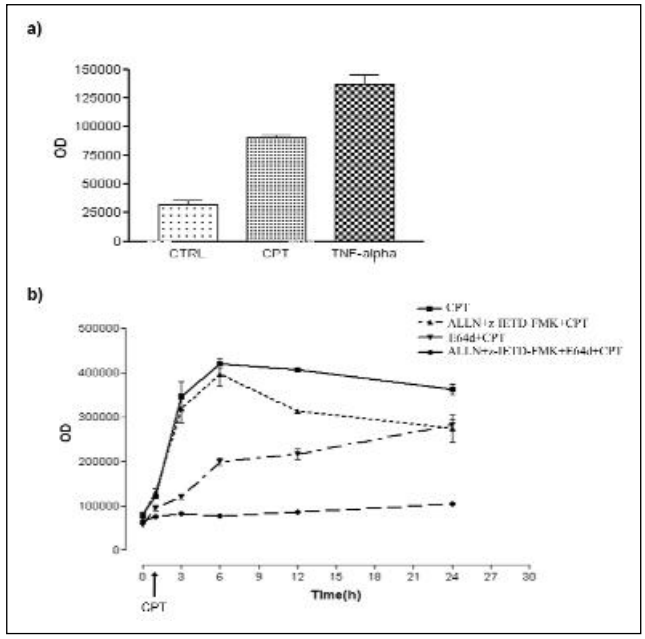

Fig. 5. a) Comparison of cathepsin B activation in CPT (0.15 μM) and TNF-α (10 ng/ml) - induced apoptosis after 60 min of cell exposure to drugs (analysis performed using cathepsin B Magic Red® substrate);
b) effect of *m*-calpain and caspase 8 inhibitors (ALLN+ z-IETD-FMK) and inhibitor of papain-like proteases (E64d) on activation and release of cathepsin B measured by optical density (OD) of red fluorescence of cathepsin B Magic Red® substrate (n=6) after CPT treatment.

The next experiment proved that activation of cathepsin B is not limited to the CPT-induced mitochondrial pathway of apoptosis, but is also characteristic of the receptor pathway of PCD I induced by TNF-α (*Fig. 5a*).

In continuation of the experiments on CPT-induced cathepsin B activation, inhibitors of *m*-calpain (ALLN), caspase 8 (z-IETD-FMK) and papain-like cysteine proteases (E64d) were applied before CPT and Magic Red® treatment. Both *m*-calpain and caspase 8 are regarded as activators of apoptosis promoters: BAX and BID, respectively (29-30). CPT alone induced a dynamic increase in cathepsin B activity reaching a plateau at 6 h after drug administration (*Fig. 5b*). Suppression of apoptosis by a combination of *m*-calpain and caspase 8 inhibitors did not significantly change the CPT-induced cathepsin B activation pattern until 6h of the experiment. After that time, the activity of cathepsin B was lower than in CPT-alone-treated cells but it was still maintained at a very high level (*Fig. 5b*). Cathepsin inhibitor (E64d) significantly delayed and diminished CPT-induced activation of cathepsin B. Activation of this enzyme in CPT-treated cultures was completely prevented by a combination of apoptotic enzyme and cathepsin inhibitors (*Fig. 5b*).

Effect of papain-like cystein protease inhibitor (E64d) on apoptosis and autophagy.

CPT administration to the incubation medium significantly increased the number of apoptotic cells, measured as a Sub-G1 region on DNA frequency distribution histograms, with a peak of cell death occurring after 1 h of cell exposure to the drug (*Fig. 6a*). Cathepsin inhibitor (E64d) abrogated the CPT-

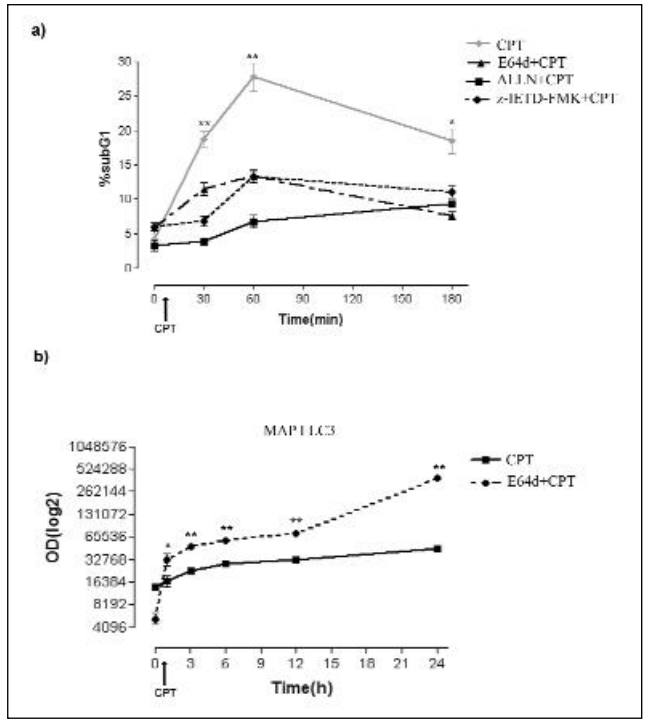

Fig. 6. a) Effect of ALLN (25 mM), z-IETD-FMK (25 μM) and E64d (15 μM) on CPT (0.15 μM) - induced apoptosis (% of cells in Sub-G1 region); *b)* Effect of papain-like protease inhibitor (E64d) on expression of MAP I LC3 in CPT-treated cultures (calculated as the optical density of MAP I LC3 protein). Each point represents the mean (± SE) from 6 replications of 3 different experiments. *- significant differences ($p \leq 0.05$), ** - highly significant differences ($p \leq 0.01$).

induced apoptosis in the examined tumor cell culture. A similar protective effect was observed when *m*-calpain and caspase 8 were inhibited with ALLN and z-IETD-FMK, respectively. The antiapoptotic effect of E64d was accompanied by a significant increase in MAP I LC3 expression after CPT (*Fig. 6b*).

BCL-2 death promoters: BAX and BID as putative cathepsin targets in CPT-induced apoptosis

It is commonly accepted that the mitochondrium is the major organelle in the apoptotic pathway and the release of mitochondrial mediators of apoptosis (cytochrome c, Smac/DIABLO, Omi/HtrA2, AIF) regulated by Bcl-2-related death agonists is regarded as a "point of no return" in the apoptotic cascade. In this experiment we examined the dependence of BAX and BID on cathepsin activity. We used LSC for quantitative analysis of BAX and BID aggregation by the measurement of MP (maximal pixel)-a parameter recommended for analysis of molecule aggregation within individual cells (31) (see Material and Methods).

The effect of cathepsin inhibition on CPT-induced BAX and BID aggregation was compared with the effect of ALLN-an inhibitor of *m*-calpain (an enzyme that is regarded as an activator of BAX) and the effect of z-IETD-FMK, an inhibitor of caspase 8 (an enzyme regarded as an activator of BID). The number of cells containing BAX and BID aggregates (cells with high MP) increased significantly

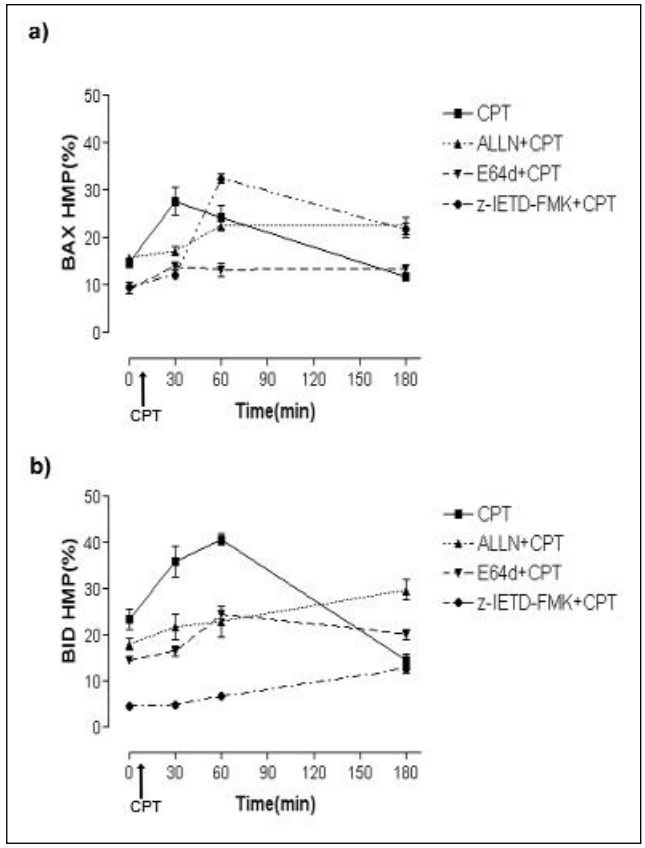

Fig.7. Effect of ALLN (25 μM), z-IETD-FMK (25 μM) and E64d (15 μM) on CPT (0.15 μM) -induced BAX (a) and BID (b) aggregation in MCF-7 cells, measured as the percent of cells with a high MP (see materials and methods). Each point represents the mean (± SE) from 6 replications.

during exposure to CPT, reaching a maximum after 30 min (BAX) or 60 min (BID) after drug administration (*Fig. 7*). The inhibitor of cathepsins (E64d) significantly abrogated CPT-induced BAX and BID aggregation. A similar effect was observed in the case of ALLN-treated cells. The inhibitor of caspase 8 (z-IETD-FMK) completely prevented CPT-induced BID aggregation (*Fig. 7b*) and delayed but did not prevent BAX aggregation (*Fig. 7a*). This may suggest that BAX aggregation is initially dependent on caspase 8, but thereafter its activation and translocation to organelle membranes (mainly mitochondrial) escapes from the influence of caspase 8.

The results obtained with LSC were confirmed by homeostatic confocal microscopy 3D reconstructions, where aggregation of BAX-GFP on mitochondria labeled with mitovector-RFP was examined in living cells exposed to CPT alone or CPT with E64d, ALLN or Z-IETD-FMK (*Fig. 8*). In control cells (0 min) BAX-GFP was evenly distributed in cytosol and punctate labeling of mitochondria (red fluorescence) was well visible. CPT supplementation into the medium evoked cell shrinkage within 6 min after administration. During 24 min of cell exposure to the

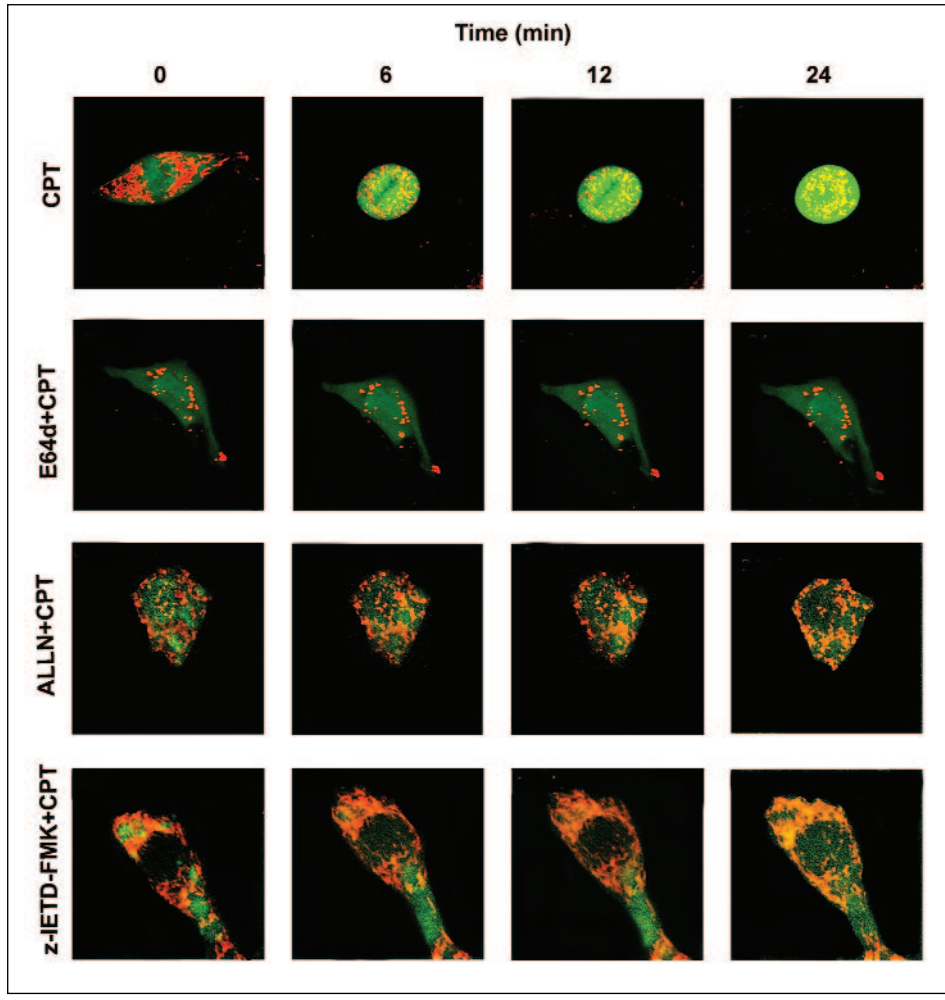

Fig. 8. Homeostatic confocal images of breast cancer MCF-7 cells exposed to: CPT (0.15 μM), CPT+E64d (15 μM), CPT+ALLN (25 μM) and CPT+z-IETD-FMK (25 μM). Cells were double transfected with: pDs mito-Red vector (red fluorescence) and pEGFP-BAX vector (green fluorescence). Aggregation of BAX on mitochondria manifested with an appearance of yellow fluorescence resulting from simultaneous excitation of both fluorescence wavelengths. Presented images are representative of at least 30 cells.

drug a gradual increase of punctate yellow fluorescence and disappearance of red fluorescence was observed. Yellow fluorescence originated from overlaying of BAX-GFP with RFP-labeled mitochondria, indicating BAX aggregation in these organelles. The inhibitor of cathepsins (E64d) completely prevented CPT-induced cell shrinkage and BAX-GFP colocalization on RFP-labeled mitochondria (*Fig. 8*). A similar effect was observed in the case of the ALLN- inhibitor of *m*-calpain, but in the case of the caspase 8 blocker (z-IETD-FMK) appearance of yellow

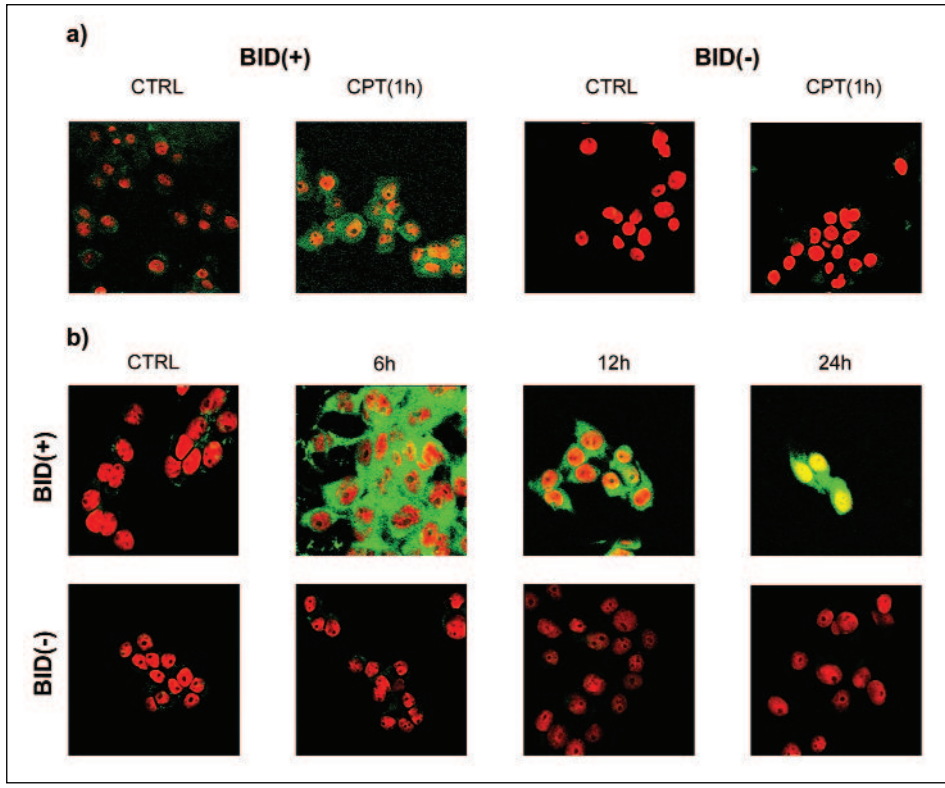

Fig. 9. a) Effect of BID silencing on BID protein content in control and CPT-treated MCF-7 cells. BID protein was labeled with Alexa 488-conjugated antibody (green fluorescence), DNA was stained with 7-aminoactinomycin D (red fluorescence); *b)* apoptotic effect of CPT (0.15 μM), measured by analysis of 89 kDa PARP degradation fragment (green fluorescence) in BID(+) and BID(-) cells. DNA was stained with 7-AAD.

fluorescence at 24 min of CPT treatment was observed, however, without any changes in the cell shape (*Fig. 8*).

BID as a molecular switch between apoptosis and autophagy in CPT-treated MCF-7 cells

The previous experiment showed that BID is a target for cathepsins in the course of CPT-induced apoptosis in breast cancer MCF-7 cells (*Fig. 7*). The RNAi technique was applied to silence *bid* gene expression (see materials and methods). In control culture of breast cancer MCF-7 cells, weak expression of BID at the protein level was observed (*Fig. 9a*). The expression of BID increased markedly within 1 h of CPT treatment. In BID (-) cells no BID protein was detected in control cultures and only a trace of BID protein in CPT-treated cultures was observed (*Fig. 9a*). BID (+) cells was able to develop apoptosis, which was shown

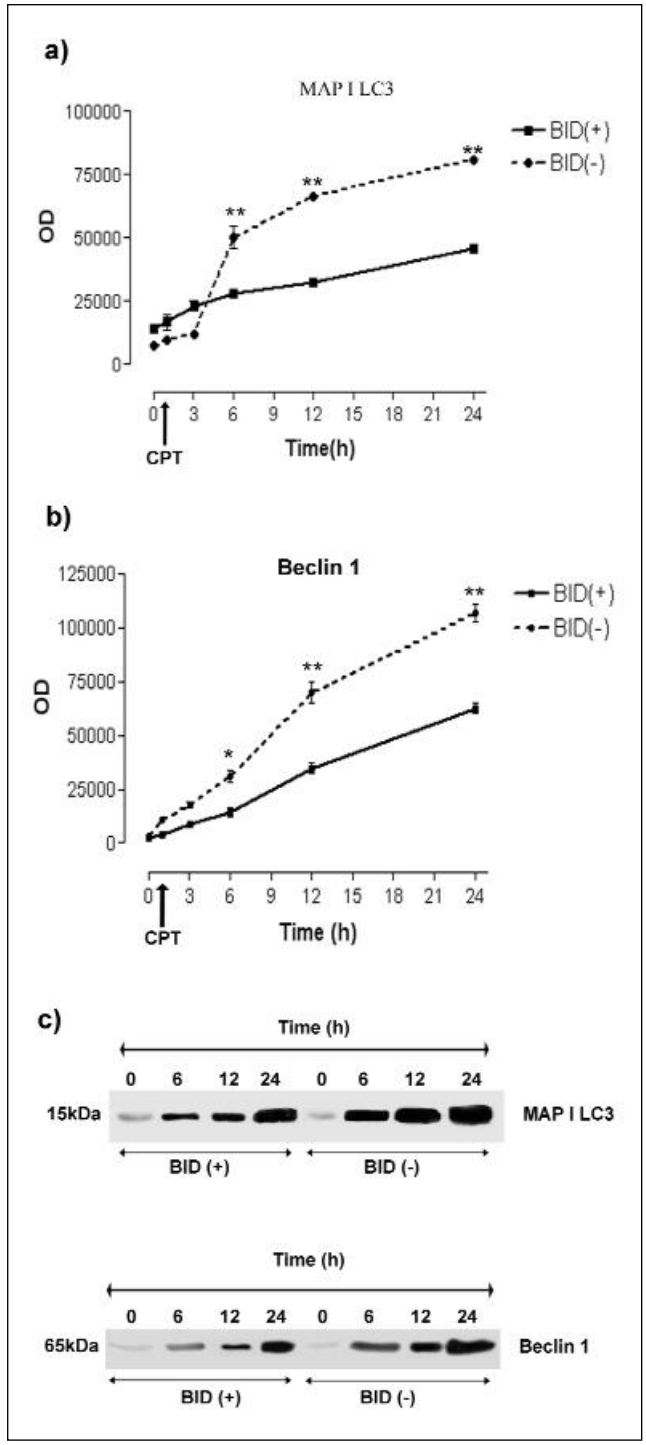

Fig. 10. Effect of BID silencing on MAP I LC3 (a) and Beclin 1 (b) protein content in control and CPT-treated MCF-7 cells. *- significant differences ($p \leq 0.05$) and **- highly significant ($p \leq 0.01$) differences n = 6. c) Western blot analysis of 15 kDa MAP I LC3 and Beclin 1 protein level in CPT - treated BID(+) and BID(-) cells.

by an increase in the content of the 89 kDa PARP degradation fragment (product of caspase 7 activity) (*Fig. 9b*). Moreover, the number of cells was dramatically reduced after 24 h CPT treatment. In BID (-) cells the 89 kDa PARP fragment was not detected, indicating effective suppression of apoptosis (*Fig. 9b*). In BID (+) cells expression of Beclin 1 and MAPI LC3 (as a marker of autophagosomes) increased progressively during 24 h of cell exposure to CPT. Significantly higher expression of Beclin1 and MAP I LC3 in BID (-) cells was observed after 6, 12 and 24 h of CPT treatment in comparison with BID (+) cells (*Fig. 10*).

DISCUSSION

The results of the present study proved that CPT induces both apoptosis (PCD I) and autophagy (PCD II) in breast cancer MCF-7 cells, however, they occur with different intensities. The program of apoptosis was rapid with a peak of apoptotic cell number observed within 60 min after drug administration (*Fig. 1*). Autophagy developed at a much slower rate with continuous progression during 24 h of cancer cell exposure to CPT (*Fig. 1*). Literature data indicate that the switch between particular types of PCD in MCF-7 cells may be related to the external death signal. Apoptosis prevails in cell cultures treated with CPT (25) or TNF-α and TRAIL (13), whereas autophagy dominates when cells are exposed to antiestrogen-tamoxifen (13, 32) or sesquiterpene analogs of taxol (33). In the later case only 10-15% MCF-7 cells exhibited elevated activity of caspase 7 as a biological marker of apoptosis (33). The results of the present study indicate that the highest coincidence of apoptosis and autophagy in CPT-treated MCF-7 cells occurs in the time interval between the third and the sixth hour of cell exposure to the drug (*Fig. 1*). Microscopic analysis of cell culture performed 6h after CPT administration revealed a number of cells with coexistence of apoptosis and autophagy. This manifested with typical morphological features of apoptosis (cell shrinkage, margination and condensation of chromatin) and autophagy (autophagosomes, autophagic vacuoles) in the same cell (*Fig. 2*). The presented results strongly suggest that autophagy is not the only alternative but can be complementary to apoptosis under the influence of CPT. The stress induced by CPT triggered both pathways of PCD in MCF-7 cells. The fast program of apoptosis rapidly eliminates the most sensitive cell subpopulations, whereas the remaining, more resistant cells develop a slower program of autophagy as a type of cell death complementary to apoptosis.

The complementarily of apoptosis and autophagy suggests mutual interconnections between both PCD pathways, however, the molecular switch still remains unidentified. Several molecular links between apoptosis and autophagy have been suggested in various cellular models, including: ASP (apoptosis-specific protein), beclin 1, Ca^{2+}/calmodulin-regulated death kinases DAPk and DRP-1, PTEN, steroid-inducible gene *E93*, signaling molecules

Akt/PKB and mTOR, and Bcl-2 family proteins (6, 32). The involvement of lysosomes in both PCD pathways (15-16, 18) may suggest involvement of cathepsins as a functional link between apoptosis and autophagy. This hypothesis was confirmed by the results of our study showing that inhibition of cathepsins by E64d, an inhibitor of papain-like cysteine proteases, resulted in significant reduction of apoptotic cell number accompanied by an increase of autophagosome formation in MCF-7 cell culture exposed to CPT (*Fig. 4*). Activation of cathepsin B during CPT-induced apoptosis belongs to the earliest events in the cell, occurring within minutes after drug administration (*Fig. 3a*). This effect is common for both the mitochondrial and death receptor pathways of apoptosis (*Fig. 3d*) and is manifested not only with activation of cathepsin B but also its subcellular redistribution to the cytosol and nucleus shown with the immunogold technique (*Fig. 3b, c*). The answer to the question whether cathepsin B activity is sufficiently stable at the neutral intracellular pH to trigger downstream apoptotic processes in the cytosol, was provided by Leist and Jaattela (18), who stated that biological fluids seem to have a stabilizing effect on cathepsin B even at neutral pH. It was shown by Guicciardi et al. (22) that cathepsin B can trigger cytochrome c release from mitochondria provided that a cytosolic extract is also added. In vitro experiments performed at neutral pH showed that papain-like cathepsins B, H, L, S and K cleave (activate) proapoptotic protein BID predominantly at Arg65 or Arg71 (14). Nonetheless, the molecular mechanisms controlling specific processes of translocating cathepsins from lysosomes to cytosol induced by the apoptotic signal still remain to be elucidated. Our study revealed that activation of cathepsin B is independent of caspase 8 and *m*-calpain, during the first 6 h of cell exposure to CPT (*Fig. 3e*). A higher activity of cathepsin B in the absence of inhibitors of caspase 8 and *m*-calpain between 6 and 24 h may suggest secondary activation of cathepsin B in late apoptotic (putrotic) cells. Stoka et al. (19) did not find evidence for direct activation of caspases by lysosomal proteases and hypothesized an indirect mode of caspase activation involving activation of BID. Suppression of apoptosis and promotion of autophagy by inhibition of papain-like cysteine proteases suggested that among molecular targets of cathepsins there are proteins that may control the balance between apoptosis and autophagy. The major candidates are proapoptotic proteins from the Bcl-2 family: BID and BAX, which are known to be activated by cathepsin B (12, 17) and cathepsin D (33), respectively. The inhibitor of papain-like cysteine proteases completely prevented BAX and BID aggregation in CPT-treated MCF-7 cells (*Fig. 5* and *6*). This may indicate the role of cathepsins in subcellular redistribution of BAX and BID. The effect of cathepsin inhibitor was comparable with the inhibitor of *m*-calpain and caspase 8 (*Fig. 5* and *6*), enzymes involved in activation of BAX and BID, respectively (29-30). It should be noticed, however, that inhibition of caspase 8 delayed CPT-induced BAX aggregation (*Fig. 5* and *6*). These results may suggest that subcellular redistribution of BAX is dependent on BID (activated by caspase 8) during the

first 30 min of CPT treatment. Activation of BAX and BID by cathepsins, caspase 8 and *m*-calpain occurs by proteolytic cleavage of an inactive protein at the N-terminal epitope with exposure of the BH3 domain. Active molecules form BAX/BID heterooligomers and translocate to the organelle membranes, mainly the outer mitochondrial membrane. There they form heteromultimeric complexes with VDAC-1 (27) functioning as a megachanel responsible for the release of apoptogenic factors (cytochrome c, Smac/DIABLO, Omi/Htr2, AIF) from the intermembrane space (25, 34-35) Mitochondria are also suggested to mediate autophagy in tumor cells (36). Our results and literature data (14, 19) strongly suggest that BID, being the major protein controlling mitochondrial membrane permeability in the course of apoptosis, may serve as a molecular switch between apoptosis and autophagy. Our hypothesis was confirmed by "knock down" of BID, which resulted in strong suppression of CPT-induced apoptosis and a shift towards autophagy, manifested with a significant increase of Beclin1 and MAP I LC3 expression (*Fig. 7*). Indirect evidence supporting involvement of BID in the switch between PCD I and PCD II was provided by Yu et al. (37), who found that autophagy was induced by caspase 8 inhibition.. Since *bid* and other proapoptotic genes undergo mutations in malignant cells (38-39) the ability of cancer cell commitment to autophagy may have important therapeutical implications

The following conclusions can be drawn: 1) autophagy is complementary to apoptosis in breast cancer MCF-7 cells exposed to CPT, 2) activation of cathepsin B is an early event independent of caspase 8 and m-calpain activity in cells exposed to apoptotic stimulus, 3) inhibition of cathepsins suppresses apoptosis and promotes autophagosome formation in CPT-treated cells, 4) a cathepsin B substrate, BID, serves as a molecular switch between apoptosis and autophagy.

Acknowledgements: This work was supported by Grants from the National Committee for Scientific Research: 117/E-385/SPB/COST/P-05/DZ 145/2002-2004 and 2 P06K 019 26.

REFERENCES

1. Lockshin RA, Osborne B, Zakeri Z. Cell death in the third millennium. *Cell Death Differ* 2000; 7: 2-7.
2. Klionsky DJ. Autophagy. Gorgetown 2004; TX: Landes Bioscience.
3. Yoshimori T. Autophagy: a regulated bulk degradation process inside cells. *Biochem Biophys Res Commun* 2004; 313: 453-458.
4. Abraham M. Death without caspases, caspases without death. *Trends in Cell Biol* 2004; 14: 184-193.
5. Meijer A, Codogno P. Regulation and role of autophagy in mammalian cells. *Int J. Biochem Cell Biol* 2004; 36: 2445-2462.
6. Ogier-Denis E and Codogno P. Autophagy: a barrier or an adaptive response to cancer. *Biochem Biophys Acta* 2003; 1603: 113-128.
7. Cuervo AM. Autophagy: in sickness and in health. *Trends in Cell Biol* 2004; 14: 70-77.

8. Mizushima N, Yamamoto A, Matsui M, Yoshimori T, Oshumi Y. In vivo analysis of autophagy in response to nutrient starvation using transgenic mice expressing a fluorescent autophagosome marker. *Mol Biol Cell* 2003; 15:1101-1111.
9. Kabeya Y, Mizushima N, Ueno T, Yamamoto A, Kirisako T, Noda T, Kominami E, Ohsumi Y, Yoshimori T. LC3, a mammalian homologue of yeast Apg8p, is localized in autophagosome membranes after processing. *EMBO J* 2000; 19: 5720-5728.
10. Nara A, Mizushima N, Yamamoto A, Kabeya Y, Oshumi Y, Yoshimori T. SKDI AAA ATPase-dependent endosomal transport is involved in autolysosome formation. *Cell Struct and Function* 2002; 27: 539-564.
11. Asanuma K, Tanida I, Shirato I, Ueno T, Takahara H, Nishitani T. MAP I LC3, a promising autophagosomal marker, is processed during differentiation and recovery of podocytes from PAN nephrosis. *FASEB J* 2003; 17: 1165-1167.
12. Kim J, Klionsky DJ. Autophagy, cytoplasm-to-vacuole targeting pathway, and pexophagy in yeast and mammalian cells. *Ann. Rev Biochem* 2000; 69: 303-342.
13. Klionsky DJ, Gregg JM, Dunn Jr, Emr SD, Sakai Y, Sandoval IV. A unified nomenclature for yeast autophagy-related genes. *Develop Cell* 2003; 5: 539-545.
14. Cirman T, Oresic K, Droga-Mazovec G, Turk V, Reed CJ, Myers RM et al. Selective disruption of lysosomes in HeLa cells triggers apoptosis, mediated by cleavage of Bid by multiple papain-like lysosomal cathepsins. *J Biol Chem* 2004; 279: 3578-3587.
15. Zhao M, Antunes F, Eaton JW, Brunk UT. Lysosomal enzymes promote mitochondrial oxidant production, cytochrome c release and apoptosis. *Eur J Biochem* 2003; 270: 3778-3786.
16. Bursh W. The autophagosomal-lysosomal compartment in programmed cell death. *Cell Death Differ* 2001; 8: 569-581.
17. Roberts LR, Adjei PN, Gores GJ. Cathepsins as effector proteases in hepatocyte apoptosis. *Cell Biochem Biophys* 1999; 30: 71-88.
18. Leist M, and Jatella M. Triggering of apoptosis by cathepsins. *Cell Death Differ* 2001; 8: 324-326
19. Stoka V, Turk B, Schendel SL, Kim TH, Cirman T, Snipas SJ et al. Lysosomal protease pathways to apoptosis. Cleavage of bid, not pro-caspases, is the most likely route. *J Biol Chem* 2001; 276: 3149-3157.
20. Bidere N, Lorenzo HK, Carmona S, Laforge M, Harper F, Dumont C et al. Cathepsin D triggers Bax activation, resulting in selective apoptosis-inducing factor (AIF) relocation in T lymphocytes entering the early commitment phase to apoptosis. *J Biol Chem* 2003; 278: 31401-31411
21. Vancompernolle K, Van Herreweghe F, Pynaert G, Van de Craen M, De Vos K, Totty N et al. Atractyloside-induced release of cathepsin B, a protease with caspase-processing activity. *FEBS Lett* 1998; 438: 150-158.
22. Guicciardi ME, Deussing J, Miyoshi H, Bronk SF, Svingen PA, Peters C et al. Cathepsin B contributes to TNF-alpha-mediated hepatocyte apoptosis by promoting mitochondrial release of cytochrome c. *J Clin Invest* 2000; 106: 1127-1137
23. Zhao M, Brunk UT, Eaton JW. Delayed oxidant-induced cell death involves activation of phospholipase A2. *FEBS Lett* 2001; 509: 399-404.
24. Zaidi AU, McDonough JS, Klocke BJ, Latham CB, Korsmeyer SJ, Flavell RA et al. Chloroquine-induced neuronal cell death is p53 and Bcl-2 family-dependent but caspase-independent. *J Neuropathol Exp Neurol* 2001; 60: 937-945.
25. Górka M, Godlewski MM, Gajkowska B, Wojewódzka U, Motyl T. Kinetics of Smac/DIABLO release from mitochondria during apoptosis of MCF-7 breast cancer cells. *Cell Biol Int* 2004; in press.
26. Godlewski MM, Motyl MA, Gajkowska B, Wareski P, Koronkiewicz M, Motyl T. Subcellular redistribution of BAX during apoptosis induced by anticancer drugs. *Anticancer Drugs* 2001; 12: 607-617.

27. Godlewski MM, Gajkowska B, Lamparska-Przybysz M, Motyl T. Colocalization of BAX with BID and VDAC-1 in nimesulide-induced apoptosis of human colon adenocarcinoma COLO 205 cells. *Anticancer Drugs* 2002; 13: 1017-1029.
28. Mizushima N. Methods for monitoring autophagy. *Int J Biochem Cell Biol* 2004; 36: 2491-2502.
29. Gao G, Dou QP. N-terminal cleavage of bax by calpain generates a potent proapoptotic 18-kDa fragment that promotes bcl-2-independent cytochrome C release and apoptotic cell death. *J Cell Biochem* 2000; 80: 53-72.
30. McDonnell JM, Fushman D, Milliman CL, Korsmeyer SJ, Cowburn D. Solution structure of the proapoptotic molecule BID: a structural basis for apoptotic agonists and antagonists. *Cell* 1999; 96: 625-634.
31. Darzynkiewicz Z, Bedner E, Smolewski P. In situ detection of DNA strand breaks in analysis of apoptosis by flow- and laser-scanning cytometry. *Methods Mol Biol* 2002; 203: 69-77.
32. Gompel A, Somai S, Chaouat M, Kazem A, Kloosterboer HJ, Beusman I et al. Hormonal regulation of apoptosis in breast cells and tissues. *Steroids* 2000; 65: 593-598.
33. Górka M, Gajkowska B, Daniewski W, łusakowska E, Godlewski MM, Motyl T. Autophagy induced by new sesquiterpene derivatives in breast cancer MCF-7 cells. Proceedings of the12th Conf. on Apoptosis, Chania, Crete, Greece 2004.
34. Mathiasen IS, Jaattela M. Triggering caspase-independent cell death to combat cancer. *Trends Mol Med* 2002; 8: 212-220.
35. Motyl T, Gajkowska B, Górka M, Godlewski MM, Lamparska-Przybysz M. Kinetics and regulation of Smac/DIABLO release from mitochondria of cancer cells exposed to apoptogenic stimulus. *Adv Cell Biol* 2004; 31: 219-233 (polish).
36. Gozuacik D, Kimchi A. Autophagy as a cell death and tumor suppressor mechanism. *Oncogene* 2004; 23: 2891-2906.
37. Yu L, Alva A, Su H, Dutt P, Freundt E, Welsh S et al. Regulation of an ATG7-beclin 1 program of autophagic cell death by caspase-8. *Science* 2004; 304: 1500-1502.
38. Lee JH, Soung YH, Lee JW, Park WS, Kim SY, Cho YG et al. Inactivating mutation of the pro-apoptotic gene BID in gastric cancer. *J Pathol* 2004; 202: 439-445.
39. LeBlanc H, Lawrence D, Varfolomeev E, Totpal K, Morlan J, Schow P et al. Tumor -cell resistance to death receptor--induced apoptosis through mutational inactivation of the proapoptotic Bcl-2 homolog Bax. *Nat Med* 2002; 8: 274-281.

Received: February 2, 2005
Accepted: May 6, 2005

Author's address: Prof. Tomasz Motyl, Ph.D., Department of Physiological Sciences, Faculty of Veterinary Medicine, Warsaw Agricultural University, Nowoursynowska 159, 02-776 Warsaw, Poland. Tel/fax: (+48) 22 847-24-52.
E-mail: t_motyl@hotmail.com